ABIOMED WORKSHOP ON ULTRASOUND IN BIOMEASUREMENTS, DIAGNOSTICS AND THERAPY,
(PP. 133-142), GDAŃSK, 7TH – 9TH SEPTEMBER 2004

PRINCIPLE, APPLICATIONS AND LIMITATIONS OF ULTRASOUND BASED ELASTOGRAPHY

H. ERMERT

Institute of High Frequency Engineering, Ruhr-University Bochum, IC 6/133, 44780 Bochum, Germany
and
Ruhr-Center of Excellence for Medical Engineering (KMR), Bochum, Germany

helmut.ermert@rub.de

1. Introduction

Mechanical properties of biological tissue are of histological relevance because of a correlation between palpable lesions (e.g. nodes) and malignant tumors. The majority of cancerous lesions can be palpated as hard inclusions, at least after they have reached a certain size. However, there are also benign changes in tissue, which tend to be harder compared to surrounding tissue. As manual palpation is limited to the skills of the examiner and contributes only subjective and qualitative information, an imaging modality could be helpful, which provides the examiner with objective and quantitative information about mechanical properties of the examined tissue.

Medical ultrasound imaging systems allow a visualization of internal mechanical tissue displacements caused by external surface forces or by induced internal forces. The spatial distribution of internal strain can be derived from tissue displacements to get so called "elastograms" [1], which lead to a visualization of both, the location and size of stiff tissue areas.

2. Elastography Principle

Elastography was introduced in 1991 as a new modality for imaging the elastic properties of biological tissue [1]. Its ability to differentiate between hard and soft tissue was used to discriminate pathological tissue [2] as well as thermally induced lesions [3].

In elastography the tissue is manually compressed with the ultrasound transducer. The basic idea is that relatively hard areas inside the tissue are compressed less than relatively soft areas. Thus local compression or strain is a measure for the tissue

elasticity. The goal of elastography is the estimation of local strain distributions from two successive ultrasound rf data frames acquired corresponding to two slightly different compression states.

The estimation of local strain values is depicted in Fig. 1. From two successive A-scans acquired at different compression states time shifts for small overlapping temporal windows can be calculated by cross-correlation techniques. Axial strains are obtained from these time shifts by using an FIR differentiation filter. This procedure is performed for every pair of a-scans of an rf-data frame set to obtain two dimensional images of the strain distribution.

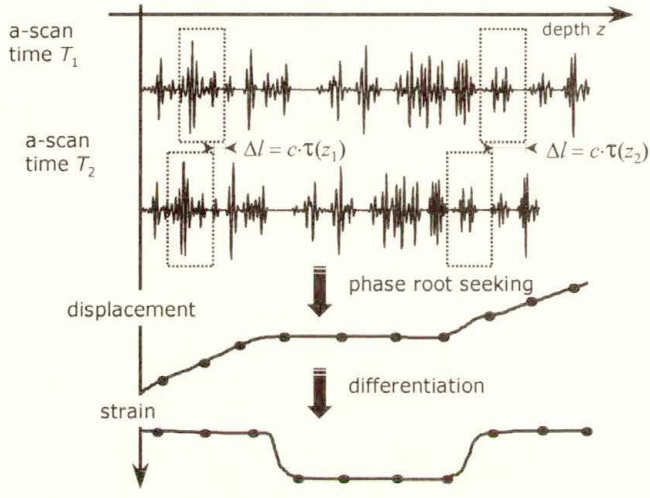

Fig. 1. Estimation of time shifts and strains from successively acquired a-scans

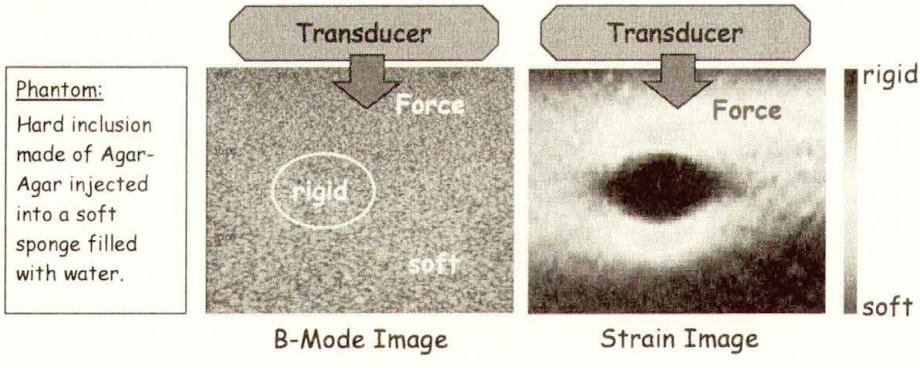

Fig. 2. Visualization of a rigid inclusion not visible in a regular B-scan image

In the resulting strain image (elastogram) stiffer regions characterized by relatively small strain values and soft regions characterized by relatively high strain values are visualized. The computation of strain images is possible in real time with a fast phase root seeking algorithm [4] on a conventional PC.

Vibrography is an extended form of elastography [5]. In this approach the transducer is moved axially in a low frequent vibrational mode of low amplitude, manual compression is not necessary. The estimation of time shifts and strain values is similar to elastography. However, the strain changes periodically from frame to frame. By filtering the periodic strain-time signals with a narrowband filter according to the frequency of compression and subsequent envelop detection stable images with good SNR can be obtained. Moreover this approach is less dependent on the experience and skills of the user.

3. Elastography Applications

Breast

With respect to the examination of breast lesions, we modified the image modalities of a conventional Siemens Sonoline™ Elegra, in order to store IQ-data from image sequences within the cine-buffer of the system and calculate elastograms offline. The compression was applied manually with the transducer. We obtained elastograms for 53 breast lesions from 48 patients [6]. In order to evaluate elastograms from malignant and benign lesions quantitatively, we measured normalized strain values within a suspect lesions (inside) and within its surrounding tissue (outside), see Fig 3.

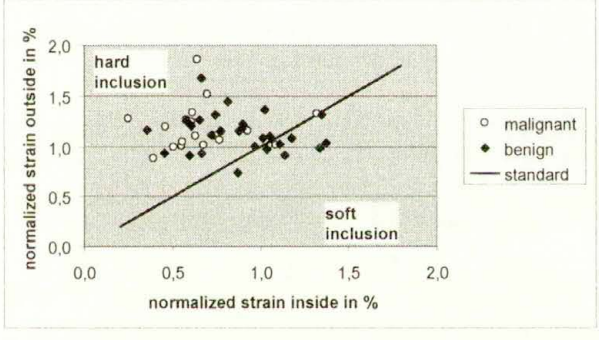

Fig. 3. Results from breast imaging: hard lesions can be expected to have lower strain values inside than outside (plotted in the upper left)

Obviously, hard lesions can be expected to have lower normalized strain values within the lesion compared to their surrounding tissue. Therefore, most of the examined lesions ended up in the upper left of the "strain plane" in Fig. 3. However, the difference in normalized strain was not significant with respect to a distinction of benign from malignant lesions in general. This might be due to the presence of a couple of fibroadenomas, which are benign tissue alterations and known to be hard, as well as carcinomas.

Prostate

A real-time version of the previously described method was implemented on a conventional Kretz Voluson 730 ultrasound system with a transrectal probe. Data was collected from 260 patients, who had to undergo radical prostatectomy due to a

prostate carcinoma, which was diagnosed in advance via needle biopsy. In addition to a digital rectal examination (DRE) and a transrectal ultrasound examination (TRU), the real-time elastography modality was applied, as well.

An example of a conventional ultrasound B-mode image, an elastogram and the corresponding histological finding is shown in Fig. 4.

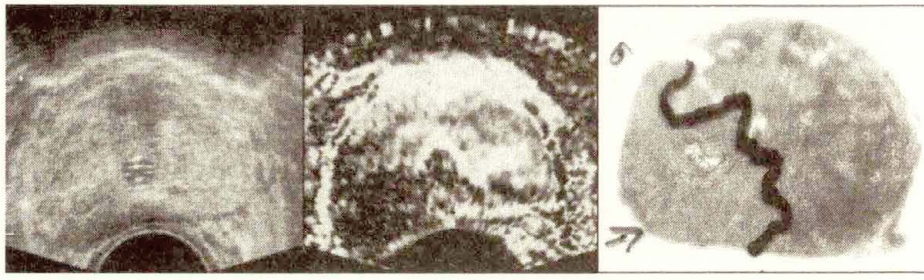

Fig. 4. B-mode image (left), elastogram (middle) and histology (right) of prostate cancer, which can be seen on the lower left of all cross sectional images. Dark regions in the elastogram correspond to hard lesions.

Histological findings showed that one third of all patient suffered from a pT2 tumor and roughly two third from a pT3 tumor. In the patient group with pT3 tumors, elastography had a positive predictive value (PPV) of 84 %, TRU of 31 % and DRE of 58 %. In the patient group with pT2 tumors, elastography had a positive predictive value (PPV) of 60 %, TRU of 31 % and DRE of 37 %.

Vessels

The clinical endpoints of arteriosclerosis, i.e. cardiovascular diseases, are still the most frequent cause of death. With respect to coronary heart disease, intravascular ultrasound (IVUS) is an invasive imaging modality to detect plaques within coronary arteries. Using a Boston Scientific Clearview IVUS machine (rotating single element transducer, 30 MHz center frequency) and a 3.2 F catheter, we obtained in-vitro results from a carotid artery, which had a plaque at 5 o'clock (see Fig. 5).

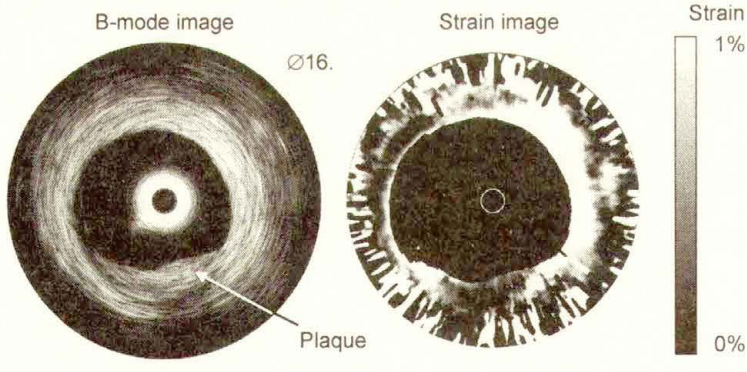

Fig. 5. B-mode IVUS image (left) and corresponding elastogram (right). Histological findings confirmed a calcified plaque at 5 o'clock.

In the elastogram there is a region with low strain values visible at 5 o'clock, which corresponds to hard tissue of a calcified plaque that was found in histology. Next to both sides of the plaque there are regions of high strain values (plaque shoulders). Note, that low strain values could also be found at 8-11 o'clock. In histology, this region was characterized as very dense tissue.

3.4. Thermotherapy Monitoring

Thermal therapy has been established as a non- or minimally invasive approach for the treatment of tumors alternative to surgical resection. Techniques used for thermal treatment include RF, laser, therapeutic ultrasound and microwaves. During a thermal therapy tissue is heated locally up to above 60° C. Cancerous tissue can thus be destroyed by coagulation.

At present there are no suitable imaging modalities available for an accurate real-time monitoring of the coagulation process. Due to the general advantages of diagnostic ultrasound (non ionizing, real-time capability, cost efficiency, ease of handling) an ultrasound based monitoring system for thermal therapies is highly desired. Initial experiments were made in vitro using porcine liver. A therapeutic rf device (Erbe Erbotom 350) and a special needle applicator for tumor treatment (Berchtold) were used. Examinations were carried out on pig liver in vitro before and after the coagulation process. Imaging of tissue samples was performed with a real-time elastography system [7]. Data was acquired using a conventional diagnostic ultrasound system (Kretz Combison 330, 7.5 MHz abdominal probe) fitted with an rf data output.

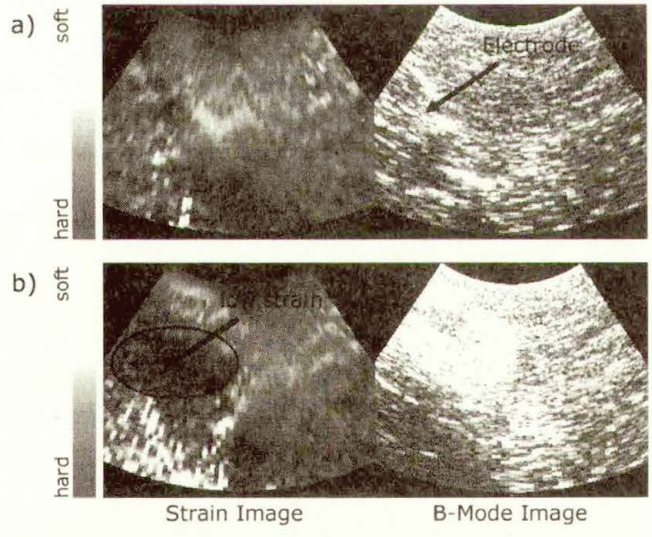

Fig. 6. Strain- and b-mode images acquired before (a) and after (b) coagulation process. The strain image in (b) shows a region of lower strain in the surrounding of the needle electrode.

The rf data was sampled by a PC ADC card (GaGe 6012, 30MHz, 12 bit). Calculation of strain images was done on a conventional PC yielding up to 7

elastograms per second. The length and overlap of the temporal windows for displacement estimation was set to 30 samples and 50 % respectively. In the resulting elastograms the coagulated zone is clearly visible as a region of low strain and therefore as a stiffer region (Fig. 6).

4. Elastography Limitations

Results from clinical studies of prostate cancer and breast cancer as well as from in vitro experiments showed that elastography has the potential to support the detection and localization of lesions as well as to support their differential diagnosis. However, it can not be overlooked that elastograms tend to have a noise appearance making it difficult to mark off the limits of hard inclusions from other tissue or artifacts, respectively. Therefore, the question arises, if there exist fundamental limits on the quality of axial strain images with respect to the examination of living tissue, which has typical values for Young's modulus from 10 to 100 kPa. We want to address this question by looking at elastography from a system theoretical point of view, shown in Fig 7.

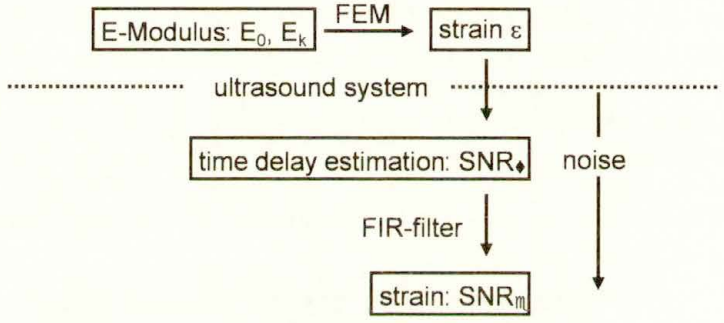

Fig. 7. Elastography from system theoretical point of view.

Given an elasticity distribution (inclusion E_k, surrounding tissue E_0), the expected axial strain can be calculated using finite element methods (FEM). Of course, the solution of the FEM problem highly depends on the elasticity distribution as well as on the boundary conditions (FEM parameters). When axial strain is measured by means of an ultrasound machine, we have to account for noise from the measurement of axial displacements (ultrasound system parameters) and noise from the calculation of axial strains (signal processing parameters). What we are interested in from an image processing point of view is the achievable contrast of elastograms SNR_ε in dependence from the mentioned parameters,

$$SNR_\varepsilon = 20 \cdot \log_{10} \frac{\varepsilon_k - \varepsilon_0}{\sigma_\varepsilon} \tag{1}$$

with ε_k being axial strain within the inclusion, ε_0 being the average strain within the whole image, which is equal to the applied rate of compression (here: ε_0 = -1 %), and σ_ε being the variance of the strain estimates. Given a certain geometry of the object (6 cm image depth, 4 cm image width), an elasticity distribution (inclusion E_k, surrounding tissue E_0) and boundary conditions (1 % compression and

Neumann conditions laterally), we can assume a plane strain state, in order to calculate strain values inside the inclusion.

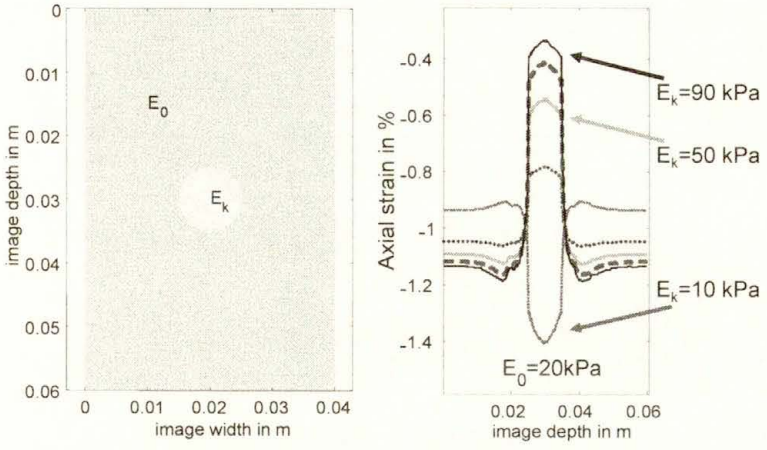

Fig. 8. Geometry of FEM analysis (left): plain strain, 1 % compression, axial strain analysis at the center of the inclusion (right).

Fig. 8 shows the geometry of our FEM analysis and the resulting axial strain values at the center of the inclusion. Note, that strain values inside the inclusion are greater than -1 %, if the inclusion is softer than the surrounding material (E_k = 10 kPa, E_0 = 20 kPa) and strain values inside the inclusion are smaller than -1 %, if the inclusion is harder than the surrounding material ($E_k > E_0$).

If we look at strain images, which are derived from time delay estimates, the quality of strain images (elastograms) is limited due to noise from the variance of time delay estimates. The variance of strain estimates σ_ε depends on the variance of time delay estimates σ_τ, the distance between two successive time delay estimates Δt and the window length T of the underlying correlation technique [8],

$$\sigma_\varepsilon^2 \geq \frac{2\,\sigma_\tau^2}{T \cdot \Delta t} \quad . \tag{2}$$

If time delays are estimated by means of an ultrasound system, i.e., broadband rf-signals, one measure of quality for time delay estimates is the Cramer-Rao-Lower-Bound (CRLB), i.e., the minimum variance that can be achieved with an unbiased time delay estimator. It has been derived by Weinstein and Weiss (1983) for time-shifted signals assuming flat signal and noise power spectra [9]. Walker and Trahey [10] derived the CRLB for time-shifted ultrasound signals,

$$\sigma_{CRLB}^2 \cong \frac{3}{2\pi^2 T\left(B^3 + 12Bf_0^2\right)}\left[\frac{1}{\rho^2}\left(1+\frac{1}{\mathrm{SNR}^2}\right)^2 - 1\right] , \tag{3}$$

in dependence from system parameters (bandwidth B, center frequency f_0, SNR of the ultrasound signals) and parameters from the correlation method (window length T, correlation coefficient ρ). Given system parameters (f_0 = 9 MHz, B = 7.2 MHz, electronic signal-to-noise ratio SNR=100) and signal processing

parameters (T = 1 μs, Δt = 0.5 μs, ρ = 0.95), we get σ_τ = 1.04 ns and σ_ε from eq. (2) turns out to be σ_ε=0.2 %.

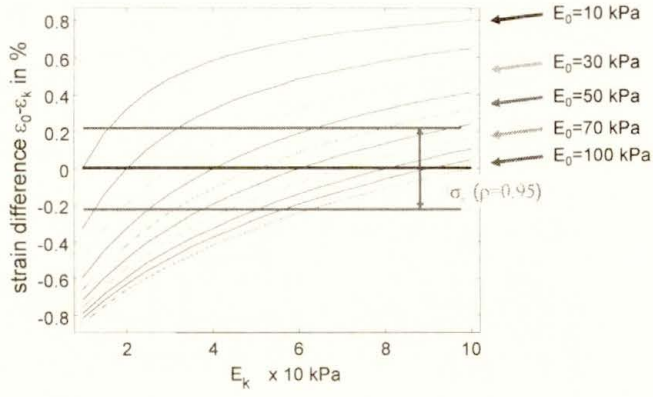

Fig. 9. Strain difference ε_0-ε_k for different values of E_k and E_0.

From Fig. 8 we can determine the mean strain value inside an inclusion ε_k for any reasonable combination of E_k and E_0, i.e., in the range of 10 kPa to 100 kPa. The result is shown in Fig. 9 and we found empirically, that the relation between E_k, E_0, ε_k and ε_0 can be linearized to

$$\frac{\varepsilon_0}{\varepsilon_k} = c_{PDE}\left(\frac{E_k - E_0}{E_0}\right) + 1 \quad . \tag{4}$$

The factor c_{PDE} can be regarded as a mechanical conversion factor and compensates for the effect of the FEM analysis (partial differential equations) on the axial strain distribution compared to a simple one-dimensional spring model, which would give c_{PDE} = 1. If we look at Fig. 9 with respect to the elastographic signal-to-noise ratio SNR_ε, we must take into account that it will take values greater than 0 dB only for pairs of E_k and E_0, which strain difference ε_0-ε_k is outside of $\pm\sigma_\varepsilon$ (here: calculated for ρ = 0.95). Substituting the result from eq. (4) into eq. (1) yields

$$SNR_\varepsilon = 20 \cdot \log_{10}\left(-\frac{\varepsilon_0}{\sigma_\varepsilon}\frac{c_{PDE}(E_k - E_0)}{E_0 + c_{PDE}(E_k - E_0)}\right) \quad . \tag{5}$$

If we focus on the detection of hard lesions, eq. (5) can be used, in order to determine, which value E_k a hard inclusion must exceed, in order to achieve an SNR_ε greater than 0 dB in dependence from a given correlation coefficient ρ (see Fig. 10).

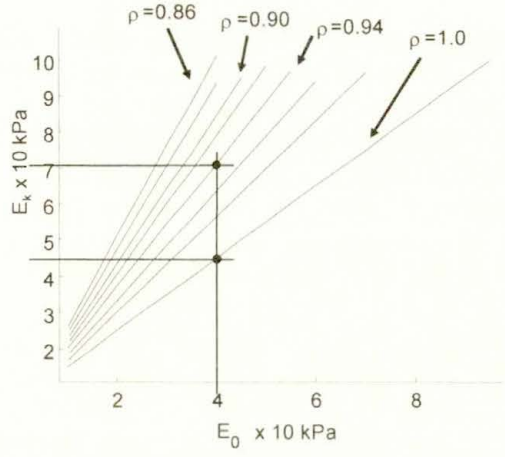

Fig. 10. Isolines ($SNR_\varepsilon = 0$ dB) for different values of correlation coefficient ρ.

E.g., for a tissue with $E_0 = 40$ kPa, a hard inclusion must have $E_k = 70$ kPa, in order to be detectable with an elastographic signal-to-noise ratio SNR_ε greater than 0 dB, given a correlation coefficient from time delay estimates of $\rho = 0.94$.

5. Conclusions

Results from clinical applications with respect to prostate and breast imaging as well as from in-vitro experiments show, that elastography has some value in medical imaging with respect to the detection, localization and differential diagnosis of hard lesions. However, strain imaging (ultrasound elastography) should be regarded as an additional imaging modality to the conventional B-mode rather than a stand-alone application. The quality of elastograms suffers from noise due the variance and decorrelation of time delay estimates, respectively. During in-vivo examinations we observed that the correlation coefficient from the underlying correlation technique takes values between 0.9 and 1.0. Introducing a mechanical conversion factor c_{PDE}, which accounts for the geometry of the object and the boundary conditions of the plane strain problem, we could show that the elastographic contrast is highly dependent of the value of the correlation coefficient. This result could be an explanation for the noisy appearance of elastograms, because the mechanical conversion factor c_{PDE} can not be greater than one, as it is not possible to amplify expected strain ratios.

Acknowledgments

Parts of the work presented in this paper are supported by the German Federal Ministry of Education and Research (bmb+f grant No. 13N8079) as projects of the Ruhr Center of Excellence for Medical Engineering (KMR), Bochum, Germany. The cooperation of our project partners

- Universitätsfrauenklinik, Knappschaftskrankenhaus BO-Langendreer (A. Jensen et al.)
- Abteilung für Kardiologie und Angiologie in den BG Kliniken Bergmannsheil Bochum (A. Mügge, W. Bojara, P. Grewe, S. Holt)
- Urologische Universitätsklinik im Marienhospital Herne (Th. Senge, H.-J. Sommerfeld, M. Garcia-Schürmann, K. Kühne)
- LP-IT Innovative Technologies GmbH, Bochum (A. Lorenz, A. Pesavento)
- Institut für Biomedizinische Technik (J. Werner, Ch. Welp)
- Institut für Hochfrequenztechnik, Ruhr-Universität (K.M. Hiltawsky, W. Khaled, C. Perrey, U. Scheipers, S. Siebers)

is greatly appreciated.

References

[1] Ophir J, Céspedes EI, Ponnekanti H, Yazdi Y, Li X. Elastography: A quantitative method for imaging the elasticity of biological tissues. Ultrasonic Imaging 1991;13:111-134.

[2] Lorenz, A.; Sommerfeld, H.J., Garcia-Schürmann, M., Philippou, S., Senge, T., Ermert, H.: "A new system for the acquisition of ultrasonic multicompression strain images of the human prostate in vivo", IEEE Trans. Ultrason. Ferroelect. Frequency Contr., vol. 46-5, pp. 1147-1154, 1999

[3] Righetti, R., Kallel, F., Stafford, R. Price, R., Krouskop, T., Hazle, J. Ophir, J.: "Elastographic Chracterization Of HIFU-Induced Lesions In Canine Livers", Ultrasound in Med. & Biol., vol. 25-7, pp 1099-1113, 1999

[4] Pesavento A, Perrey C, Krueger M, Ermert H. A Time-Efficient and Accurate Strain Estimation Concept for Ultrasonic Elastography Using Iterative Phase Zero Estimation. IEEE Trans. Ultrason. Ferroelect. Frequency Contr. 1999;46:1057-1067.

[5] Pesavento, A., Lorenz, A., Siebers, S., Ermert, H.: "New real-time strain imaging concepts using diagnostic ultrasound", Phys. Med. Biol., vol. 45, pp. 1423-1435, 2000

[6] Hiltawsky KM, Krueger M, Starke C, Heuser L, Ermert H, Jensen A. Freehand Ultrasound Elastography of Breast Lesions: Clinical Results. Ultrasound in Medicine and Biology 2001; 27(11):1461-1469.

[7] Pesavento A, Lorenz A, Ermert H. System for real-time elastography. Electronics Letters 1999;35(11):941-942.

[8] Céspedes EI, M. Insana, J. Ophir. Theoretical Bounds on Strain Estimation in Elastography. IEEE Trans. Ultrason. Ferroelect. Frequency Contr. 1995;42:969-972.

[9] Weinstein E, Weiss AJ. Fundamental Limitations in Passive Time Delay Estimation – Part II: Wide-Band Systems. IEEE Trans. Acoust., Speech, Sig. Proc. 1983; 31:1064-1078.

[10] Walker WF, Trahey GE. A Fundamental Limit on the Accuracy of Speckle Signal Alignment. IEEE Ultrasonics Symposium 1994; 1787-1791.